

## 2D steady-state thermal analysis of a line-start, permanent magnet synchronous motor

**Abstract.** The presented paper contains an analysis of heat transfer in a low power electric motor. A numerical model is presented together with its empirical verification. The model includes mixed convection as well as heat diffusion in motor's frame. Steady-state conditions at constant rated load were investigated. Frame surface temperature distribution obtained using CFD was compared with measurements conducted using thermocouples. Comparison between measured and calculated temperatures allows for an assessment of accuracy of the presented numerical model.

**Streszczenie.** Artykuł zawiera analizę wymiany ciepła w silniku synchronicznym wzbudzonym magnesami trwałymi i rozruchem bezpośrednim małej mocy. Zaprezentowano model numeryczny oraz jego weryfikację eksperymentalną. W obliczeniach uwzględniono konwekcję mieszaną oraz dyfuzję ciepła wewnątrz maszyny. Wyniki obliczeń temperatury na powierzchni silnika porównano z pomiarami wykonanymi przy pomocy termopar. Porównanie wyników pomiarów i obliczeń pozwala na ocenę dokładności modelu numerycznego. (Dwuwymiarowa analiza ustalonego stanu cieplnego silnika synchronicznego wzbudzonego magnesami trwałymi i rozruchu bezpośrednim)

**Keywords:** synchronous motor, permanent magnets, line-start, thermal analysis, computational fluid dynamics

**Słowa kluczowe:** silnik synchroniczny, magnesy trwałe, rozruch bezpośredni, analiza termiczna, obliczeniowa mechanika płynów

### Introduction

Majority of the materials used in construction of electrical machines exhibit a significant change of their physical properties with temperature. As a result, changes of temperature influence electromechanical features such as efficiency or electromagnetic torque. Thus, thermal analysis can improve the accuracy of electromagnetic calculations [1].

Another important aspect which should be considered during design is the impact of temperature on stability of the winding insulation. Operational temperature of the machine is directly related to the insulation's durability [2]. Therefore, an important task is to determine the temperature distribution inside a running motor.

The most popular methods of calculation are lumped parameter thermal network and Finite Element Method. The two methods have a different grade of discretization. Hence, thermal network provides faster calculations at the expense of accuracy, thanks to a much smaller number of nodes. Finite Element Method grants more accurate results and gives a deeper insight into the thermal phenomena occurring in the machine, yielding a detailed temperature distribution. However, the accuracy of both methods depends on the precision of determining boundary conditions – mainly the heat transfer coefficient on the surface of the motor's frame [3]. It can be determined using either of the following methods: on the basis of semi-empirical equations or computational fluid dynamics.

The use of semi-empirical equations requires an introduction of a number of simplifying assumptions [4]. Therefore, these equations have limited accuracy and may bring unsatisfactory results. A method free of these disadvantages is the usage of Computational Fluid Dynamics. Solving flow equations using Finite Volume Method in a 3D domain allows for calculations of volume flow of air induced by a fan. On this basis, it is possible to simultaneously determine distribution of heat transfer coefficient on the surface of the motor. In order to take advantage of the most accurate methods available at the design stage, calculations of temperature distributions using FEM and CFD have been conducted. The results of the calculations were verified using measurements performed on a physical model.

### Numerical model

In order to determine the temperature distribution inside the motor it is necessary to define volumetric heat sources and boundary conditions. An electromagnetic model pro-

vides information about the sources, whereas CFD calculations grant heat transfer coefficient distribution on surface of the motor, which can be applied as a boundary condition. Finally, after incorporating data from previous simulations into a thermal model, heat diffusion equation can be solved inside the motor.

### Electromagnetic model

Heat dissipation occurring in the machine is computed for a model of a Line-Start Permanent Magnet Synchronous Motor, which has a stator and mechanical construction of the induction motor type Sh90 L-4. Considered motor has a different rotor, in which permanent magnets are buried inside the rotor and complemented by a starting cage. The 2D numerical model used for the calculations is based on the following partial differential equation:

$$(1) \nabla \times \frac{1}{\mu} \times \nabla A = J_s - \sigma \nabla V + \nabla \times H_c + \sigma v \times \nabla \times A,$$

where:  $\mu$  – magnetic permeability,  $A$  – magnetic vector potential,  $J_s$  – source current density,  $\sigma$  – electric conductivity,  $V$  – electric potential,  $H_c$  – coercivity of the permanent magnet,  $v$  – linear velocity [5].

Rated operating conditions of the motor of 400 V symmetrical three-phase voltage, 50 Hz frequency and a constant load equal 1900 W were assumed. Zero normal component of the vector potential was taken as the boundary condition on the outer envelope of the stator. As a result of the discretization, an unstructured mesh consisting of 16 378 elements has been obtained.

### Computational fluid dynamics model

In order to determine the distribution of heat transfer coefficient on the surface of the motor it is necessary to compute the air flow field around it. To achieve this, a three-dimensional geometry of the fan and motor has been prepared, incorporating some justifiable simplifications. Omission of small details of geometry allows for creation of a better quality mesh while maintaining a given number of elements. It is a compromise between accuracy and required computational effort. The model uses two reference systems (Multi Reference Frame). The first, stationary, domain covers the fluid around the machine. The second domain encompasses the fluid surrounding the fan. For each of the domains a separate mesh was created, both of which combined cover the whole considered domain.

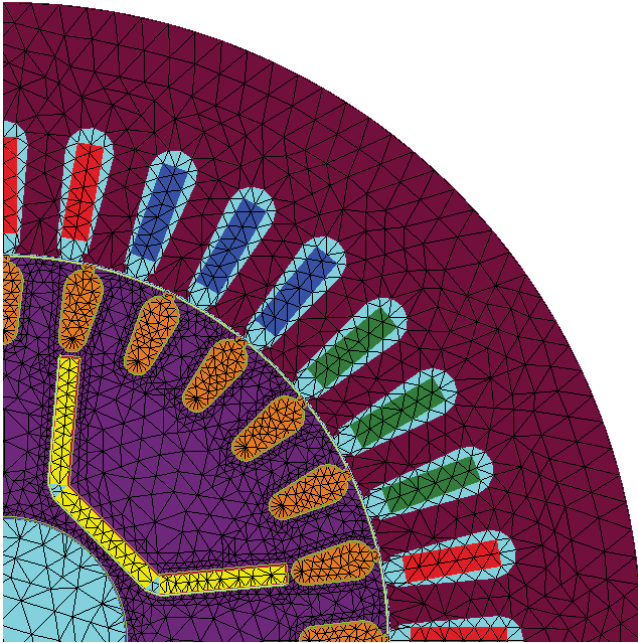


Fig. 1. A quarter of the mesh supplied to the electromagnetic calculations

For the domain associated with the rotating frame of reference the thickness of the fan was neglected. A structural grid composed of about 260 000 hexahedral elements was created. A no-slip boundary condition was assumed at the walls of the fan. Furthermore, it was assumed, regarding the energy equation, that the surface is adiabatic.



Fig. 2. Cross-section of the domain associated with the fixed reference system

The volume associated with the fixed reference frame was discretized using an unstructured tetrahedral mesh. It was decided to follow this path, due to difficulties with building block structure for such a complex geometry. This domain constitutes a cuboid with volumes of the motor and the rotating domain deducted.

A no-slip boundary condition was assumed for velocity field on the walls of the motor from the fluid side. Additionally, it was assumed that the surfaces transferring heat (ribbed body, bearing shields) are isothermal. Other areas were assumed to be adiabatic. Calculations were carried out for air pressure of 1013.25 hPa and a temperature of 20°C. The following set of PDEs was solved:

$$(2) \quad \frac{\partial \rho}{\partial t} + \nabla(\rho \mathbf{U}) = 0,$$

$$(3) \quad \frac{\partial(\rho \mathbf{U})}{\partial t} + \nabla(\rho \mathbf{U} \otimes \mathbf{U}) = -\nabla p + \nabla \tau,$$

$$(4) \quad \frac{\partial(\rho h)}{\partial t} - \frac{\partial p}{\partial t} + \nabla(\rho \mathbf{U} h) = \nabla(\lambda \nabla T) + \nabla(\mathbf{U} \tau) + S_E,$$

where:  $\mathbf{U}$  – vector of velocity,  $\rho$  – fluid density,  $h$  – specific total enthalpy,  $p$  – static pressure,  $\lambda$  – thermal conductivity,  $T$  – temperature,  $\tau$  – shear stress,  $S_E$  – energy source term [6], [7].

Turbulence was accounted for using a RANS model, namely the SST variation of the  $k - \omega$  model. Radiation has been neglected, given a relatively narrow temperature margin between the participating surfaces of the motor and the surroundings.

On the basis of the numerical solution of the above equations in the given domain, it is possible to calculate the distribution of the heat transfer coefficient on the motor's surface. These results can be used to compute heat transfer inside the motor.

### Heat diffusion model

In order to determine the temperature distribution a two-dimensional model of the motor was created. Heat diffusion equation was solved over this domain, taking into account the volumetric heat sources and using a third type boundary condition. Geometry of the motor has been created on the basis of the electromagnetic model and completed with the ribbed frame. This allowed for usage of the boundary conditions obtained using CFD, without a need to calculate the thermal resistance of the frame. The stator windings have been replaced by a single lump, characterized by a constant conductivity. Its value was calculated using homogenization technique [8]. Geometry of permanent magnets was simplified in similar way. Thermal resistances at the interface between the individual elements were taken into account through an equivalent air gap. The mesh consists of approximately 30 000 triangular elements (Fig. 3).

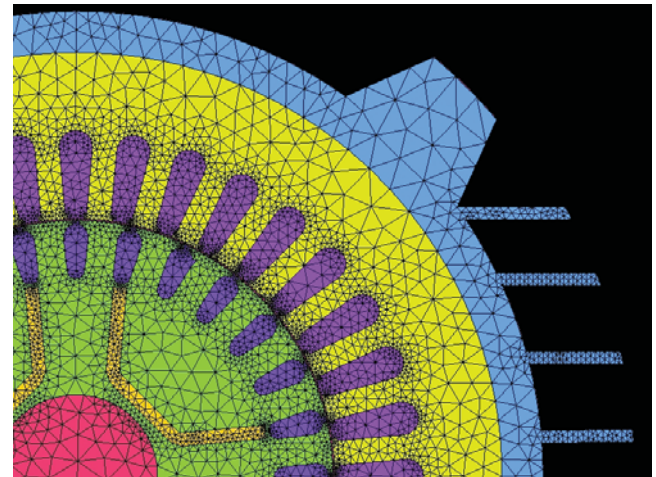


Fig. 3. Mesh obtained for the purpose of heat transfer calculations

The following PDE was solved [9]:

$$(5) \quad \frac{\partial(\rho h)}{\partial t} + \nabla(\rho \mathbf{U} h) = \nabla(\lambda \nabla T) + S_E,$$

### Results

First of all, electromagnetic calculations were performed at the pre-established temperatures of individual parts. This has provided information about the heat dissipated in the core (Fig. 4), stator windings and rotor cage. The aggregate values are equal 52 W, 156 W and 17 W, respectively.

In the next step, calculations of air flow induced by a fan have been carried out, in order to obtain the heat transfer coefficient distribution on the frame's surface. For the purpose of further calculations, resulting values were averaged, yielding  $h_{avg} = 38.5 \text{ W/m}^2\text{K}$ . This value was subsequently supplied to the thermal analysis.

However, it could not be substituted directly, since the heat transfer area exceeds twice the product of the outer perimeter and the length of the package. Therefore, the value used in the 2D calculations was determined by multiplication of the average convective heat transfer coefficient by the ratio of the actual surface area to the heat transfer area corresponding to the length of the package.

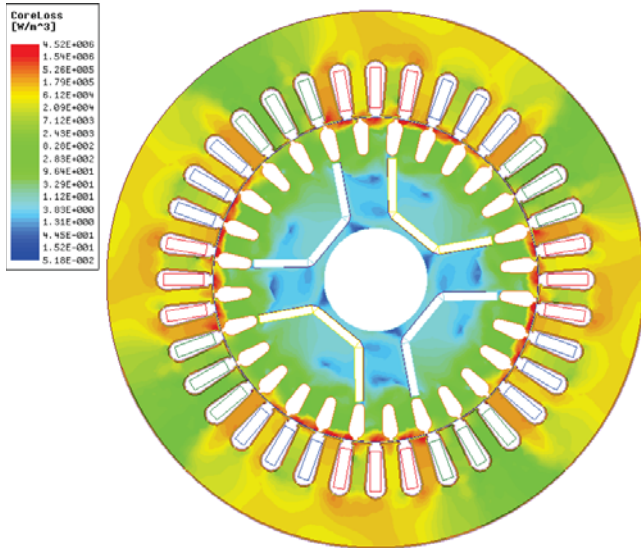


Fig. 4. Heat dissipation in the motor's core at rated load (logarithmic scale)

$$(6) \quad h_0 = h_{avg} \frac{A_C}{BL},$$

where:  $A_C$  – total area of the frame,  $B$  – outer perimeter of the body,  $L$  – lamination length. Knowledge of this variable allowed for the thermal analysis of the motor's interior in a steady state.

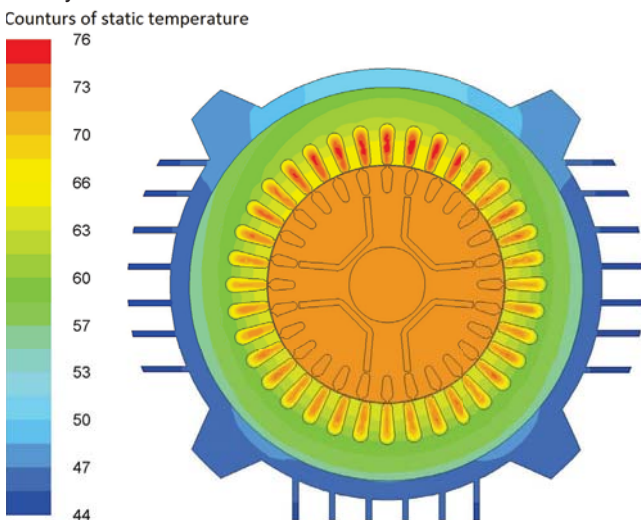


Fig. 5. Temperature distribution inside the motor

### Models' validation

In order to verify the results yielded by the electromagnetic model, measurements of current, voltage and torque

have been performed at a constant rated load in a steady state using the direct method. Comparison of the electromechanical quantities obtained on empirical and numerical basis is shown in Table 1.

Table 1. Validation of the electromagnetic model

Quantity	$U$	$I$	$P_1$	$P_2$	$\eta$	$\cos\varphi$
Unit	V	A	W	W	-	-
Empirical	400	3.37	1892	2177	0.869	0.93
Numerical	400	3.19	1884	2109	0.893	0.95

The observed differences, amounting up to a few percent, may be attributed to an a priori assumption of the engine's operating temperature. Accuracy could be improved by an iterative solution of the thermal model, update of the material properties on the basis of the obtained temperature distribution and recalculation of the volumetric heat sources. Such a procedure should be carried out until no significant changes occur.

Validity of thermal model is confirmed by comparison the results of thermal modeling with empirical data (Table 2). The temperatures of the fixed parts were measured using a set of type K thermocouples (Fig. 6), whereas the temperature of the rotor was measured using a pyrometer installed in the end shield (Fig. 7).

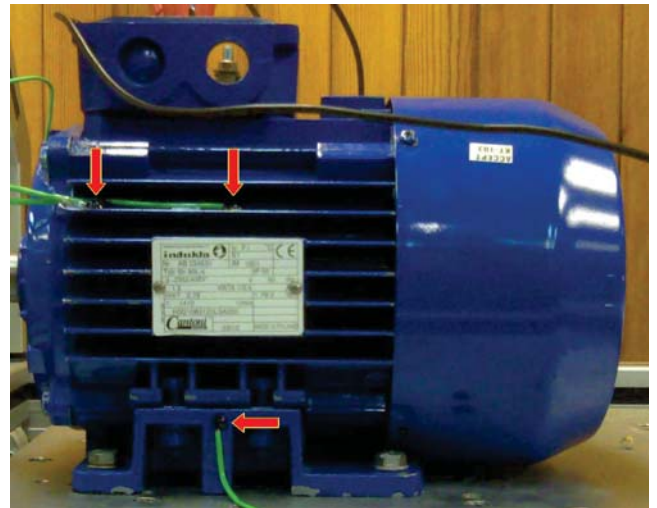


Fig. 6. Mountings of thermocouples

Table 2. Validation of the thermal model

Location		End of a rib	Middle of a rib	Windings	Rotor
$T$ – Empirical	$^{\circ}\text{C}$	41.1	42.5	68.1	71.1
$T$ – Numerical	$^{\circ}\text{C}$	43.6	43.6	70.5	72.4

### Conclusions

Calculations of heat dissipation performed using a two-dimensional model are characterized by a satisfactory accuracy and can successfully be utilized in the design process of electrical machines. One of their main advantages is the short calculation time, usually not exceeding 10 s. Improvement of solution's accuracy, particularly regarding electromechanical parameters, can be achieved either through coupling of thermal and electromagnetic calculations or their iterative repetition.

The approach presented in the article does not provide full information about the temperature distribution in the machine. The bearings and winding end connection have been

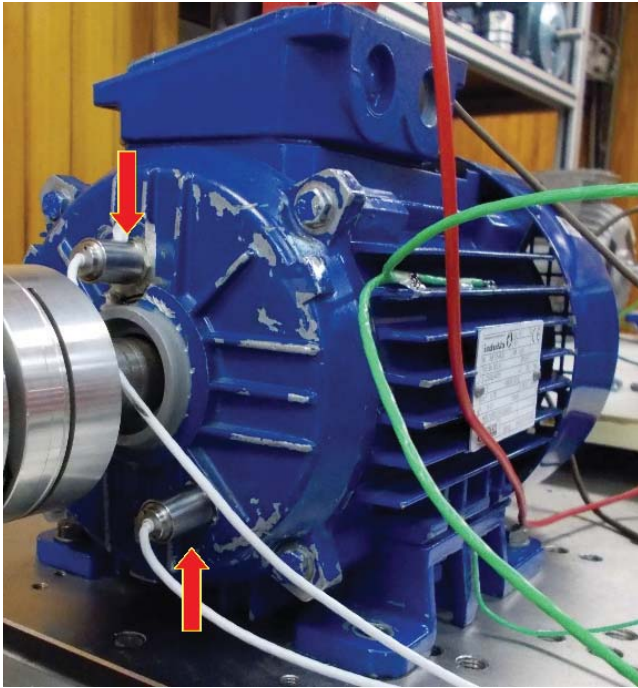


Fig. 7. Mountings of pyrometers

omitted. Determination of their temperatures is possible on the basis of three-dimensional calculations. Therefore, further development the model has been envisioned, ultimately leading to creation of a three-dimensional thermal model, coupled with a two-dimensional electromagnetic model.

#### Acknowledgments

Calculations have been carried out using resources provided by Wrocław Centre for Networking and Supercomputing (<http://wcss.pl>), grant No. 390.

**Authors:** M. Sc. Szymon Lipiński, Ph. D. Jan Zawilak, Faculty of Electrical Engineering, M. Sc. Krzysztof Grunt, Faculty of Mechanical and Power Engineering, Wrocław University of Technology, ul. Wyspiańskiego 27, 50-370 Wrocław, Poland, email: [krzysztof.grunt@pwr.edu.pl](mailto:krzysztof.grunt@pwr.edu.pl), [szymon.lipinski@pwr.edu.pl](mailto:szymon.lipinski@pwr.edu.pl), [jan.zawilak@pwr.edu.pl](mailto:jan.zawilak@pwr.edu.pl)

#### REFERENCES

- [1] Lefik M.: Design of permanent magnet synchronous motors including thermal aspects, *COMPEL: The International Journal for Computation and Mathematics in Electrical and Electronic Engineering*, 34, pp. 561–572, 2015.
- [2] Faharani M., Gockenbach E., Borsi H., Schäfer K., Kauffhold M.: Behavior of Machine Insulation Systems Subjected to Accelerated Thermal Aging Test, *IEEE Transactions on Dielectrics and Electrical Insulation*, 17(5), pp. 1364–1372, 2010.
- [3] Boglietti A., Cavagnino A., Staton D., Shanel M., Mueller M., Mejuto C.: Evolution and Modern Approaches for Thermal Analysis of Electrical Machines, *IEEE Transactions on Industrial Electronics*, 56(3), pp. 871–882, 2009.
- [4] Çengel Y., Ghajar A.: *Heat and Mass Transfer Fundamentals & Applications*, McGraw Hill Education, 5th edition, Chapter Five: External Forced Convection, pp. 307–378, 2015.
- [5] ANSYS Maxwell 16.2: Maxwell 2D Technical Notes – Transient Simulation, Maxwell Online Help
- [6] ANSYS CFX 16.2: CFX Modelling Guide & Theory Guide, ANSYS Help Viewer
- [7] Menter F. R., Kuntz M., Langtry R.: Ten years of industrial experience with the SST turbulence model, *Turbulence, Heat and Mass Transfer 4*, Begell House Inc., 2003.
- [8] Mynarek P., Kowol M.: Metoda homogenizacji uzwojeń wysypowanych w maszynach elektrycznych, *Maszyny Elektryczne – Zeszyty Problemowe*, Nr 1/2015 (105), pp. 149–154, 2015.
- [9] ANSYS Fluent 16.2: Fluent Theory Guide, ANSYS Help Viewer